frontiers | Frontiers in Plant Science

TYPE Original Research
PUBLISHED 04 January 2023
DOI 10.3389/fpls.2022.1091115

Check for updates

OPEN ACCESS

EDITED BY
Shizue Matsubara,
Forschungszentrum Jülich, Germany

REVIEWED BY
Daisuke Sugiura,
Nagoya University, Japan
Berkley James Walker,
Michigan State University,
United States

*CORRESPONDENCE
Johannes Kromdijk
Wannekromdijk@gmail.com

SPECIALTY SECTION
This article was submitted to Crop and Product Physiology, a section of the journal Frontiers in Plant Science

RECEIVED 06 November 2022
ACCEPTED 05 December 2022
PUBLISHED 04 January 2023

CITATION
Arce Cubas L, Vath RL, Bernardo EL, Sales CRG, Burnett AC and Kromdijk J (2023) Activation of CO_2 assimilation during photosynthetic induction is slower in C_4 than in C_3 photosynthesis in three phylogenetically controlled experiments. *Front. Plant Sci.* 13:1091115. doi: 10.3389/fpls.2022.1091115

COPYRIGHT
© 2023 Arce Cubas, Vath, Bernardo, Sales, Burnett and Kromdijk. This is an open-access article distributed under the terms of the Creative Commons Attribution License (CC BY). The use, distribution or reproduction in other forums is permitted, provided the original author(s) and the copyright owner(s) are credited and that the original publication in this journal is cited, in accordance with accepted academic practice. No use, distribution or reproduction is permitted which does not comply with these terms.

Activation of CO_2 assimilation during photosynthetic induction is slower in C_4 than in C_3 photosynthesis in three phylogenetically controlled experiments

Lucía Arce Cubas[1], Richard L. Vath[1], Emmanuel L. Bernardo[1,2], Cristina Rodrigues Gabriel Sales[1], Angela C. Burnett[1] and Johannes Kromdijk[1]*

[1]The University of Cambridge, Department of Plant Sciences, Cambridge, United Kingdom, [2]University of the Philippines Los Baños, Institute of Crop Science, College of Agriculture and Food Science, College, Laguna, Philippines

Introduction: Despite their importance for the global carbon cycle and crop production, species with C_4 photosynthesis are still somewhat understudied relative to C_3 species. Although the benefits of the C_4 carbon concentrating mechanism are readily observable under optimal steady state conditions, it is less clear how the presence of C_4 affects activation of CO_2 assimilation during photosynthetic induction.

Methods: In this study we aimed to characterise differences between C_4 and C_3 photosynthetic induction responses by analysing steady state photosynthesis and photosynthetic induction in three phylogenetically linked pairs of C_3 and C_4 species from *Alloteropsis*, *Flaveria*, and *Cleome* genera. Experiments were conducted both at 21% and 2% O_2 to evaluate the role of photorespiration during photosynthetic induction.

Results: Our results confirm C_4 species have slower activation of CO_2 assimilation during photosynthetic induction than C_3 species, but the apparent mechanism behind these differences varied between genera. Incomplete suppression of photorespiration was found to impact photosynthetic induction significantly in C_4 *Flaveria bidentis*, whereas in the *Cleome* and *Alloteropsis* C_4 species, delayed activation of the C_3 cycle appeared to limit induction and a potentially supporting role for photorespiration was also identified.

10.3389/fpls.2022.1091115

Discussion: The sheer variation in photosynthetic induction responses observed in our limited sample of species highlights the importance of controlling for evolutionary distance when comparing C_3 and C_4 photosynthetic pathways.

KEYWORDS

C_4 photosynthesis, C_3 photosynthesis, photosynthetic induction, CO_2 assimilation, photorespiration, non-steady state, light response

Introduction

Photosynthesis is the foundation of life on earth, the source of food, oxygen, and most of our energy. A particularly successful adaptation to the ancestral form is C_4 photosynthesis, which despite its complexity has independently arisen in at least 66 lineages of angiosperms and appeared in 19 unrelated plant families (Sage, 2004; Kellogg, 2013). Although only 3% of flowering species use the C_4 pathway, C_4 species represent 23% of global carbon fixation (Still et al., 2003), and maize and sugar cane are two of the four crops that account for half of the world's crop production (FAO, 2020). Despite the undeniable importance of C_4 species, there is comparatively less focus on improving C_4 performance – photosynthetic induction has consistently been flagged as a source of inefficiency in C_4 species relative to C_3 ones (Sage and McKown, 2006; Slattery et al., 2018; Sales et al., 2021), yet a lack of knowledge on the specifics of the C_4 induction response persists due to limited understanding of variation in photosynthetic induction between C_3 and C_4 photosynthesis, as well as across different C_4 species.

Most C_4 species display 'Kranz' anatomy, in which mesophyll (M) and bundle sheath (BS) cells are arranged concentrically around the leaf veins. Unlike in C_3 species, where initial CO_2 fixation and assimilation processes occur within the same cell, in C_4 species these activities are typically partitioned between M and BS cells. In the cytosol of M cells, equilibrium between CO_2 and bicarbonate is rapidly established by carbonic anhydrase. Bicarbonate is then fixed by phosphoenolpyruvate carboxylase (PEPC) into 4-carbon molecules that are further reduced before diffusing into the BS, where they are decarboxylated to release CO_2 around ribulose 1,5-biphosphate carboxylase/oxygenase (Rubisco), the central enzyme in carbon fixation (Leegood, 2002). The C_4 carbon concentrating mechanism (CCM) thus enhances photosynthesis and suppresses Rubisco's oxygenase activity and resulting photorespiration – the phospho-glycolate salvaging pathway that consumes energy and reducing equivalents, and releases CO_2. However, the operation of the CCM has an energetic cost, and C_4 species require additional ATP for PEP regeneration on top of the energetic demands of the C_3 cycle (Yin and Struik, 2018).

The increased efficiency of the C_4 pathway relative to the C_3 ancestral state is especially apparent under constant high light (Wang et al., 2012). However, during changes in light intensity, some C_4 species display impaired carbon assimilation in comparison to C_3 species (Kubásek et al., 2013; Slattery et al., 2018; Li et al., 2021). Decreases in photosynthetic efficiency during light induction (in response to an increase in light intensity) occur irrespective of photosynthetic pathway and are often explained by lags in regeneration of ribulose-1,5-biphosphate (RuBP) within the C_3 cycle, Rubisco activation, and stomatal opening (Pearcy and Seemann, 1990; Pearcy, 1990; Sassenrath-Cole and Pearcy, 1992; Mott and Woodrow, 2000). In addition, C_4 photosynthesis requires synchronous operation of C_3 and C_4 cycles and any loss of coordination during induction could lead to reduced efficiency of carbon fixation in C_4 species. Faster activation of the CCM relative to C_3 cycle activation in the BS may result in diffusional leakage of highly concentrated CO_2 out of the permeable BS back into M cells and a raised energetic cost for CO_2 assimilation, as recently suggested by Wang et al. (2022) and Lee et al. (2022). A 30-60% increase in BS leakiness of CO_2 during photosynthetic induction relative to steady state photosynthesis has been identified in maize and sorghum (Wang et al., 2022). This suggests that the C_3 cycle in some C_4 species is slower to activate than the C_4 CCM. Alternatively, the C_4 cycle could be the limiting factor during induction due to the need to build up metabolite gradients for the shuttling of CCM intermediates between M and BS cells. If so, the reduced supply of CO_2 to the BS would lead to weaker suppression of photorespiration, and a temporary disconnect between photosynthetic electron transport and CO_2 fixation (Sage and McKown, 2006; Kromdijk et al., 2010; Slattery et al., 2018). Although incomplete suppression of photorespiration can reduce photosynthetic efficiency, photorespiratory metabolite pools have also been suggested to help prime the C_4 cycle (Kromdijk et al., 2014; Stitt and Zhu, 2014; Schlüter and Weber, 2020; Medeiros et al., 2022). Higher relative

photorespiratory rates appear to occur under low light and during photosynthetic induction (Kromdijk et al., 2010; Medeiros et al., 2022); the resulting photorespiratory intermediates could act as a carbon reservoir from which to build C_3 and C_4 metabolite pools (Fu and Walker, 2022). The presence of an endogenous source of carbon is supported by the inability to account for the net increase in C_3 and C_4 cycle intermediates during light induction based on rates of CO_2 assimilation alone (Leegood and Furbank, 1984; Usuda, 1985).

Whilst the experimental evidence and putative mechanisms detailed above may indeed suggest that C_4 species could be more affected by transient decreases in photosynthetic efficiency during induction relative to steady state than C_3 species, most of the work does not directly compare C_3 and C_4 species in a common experiment, but instead often focuses on a single species, such as maize (Zelitch et al., 2009; Kromdijk et al., 2010; Medeiros et al., 2022). Some direct comparisons between C_3 and C_4 photosynthesis have been made in sets of contrasting grass species (Lee et al., 2022) and species within the same genus (Kubásek et al., 2013), but so far the only C_3 and C_4 species studied that share a relatively recent common ancestor are *Flaveria* (Li et al., 2021). Phylogenetic distance can strongly confound the apparent photosynthetic differences observed (Taylor et al., 2010) and to confirm whether observed differences are due to photosynthetic pathway or evolutionary variation, studies conducted on phylogenetically linked C_3 and C_4 species are necessary. Furthermore, despite striking similarities in the anatomy and biochemistry of C_4 species from diverse evolutionary origins, there is still great diversity amongst species. Some common variations are the main decarboxylases utilised to release CO_2 in BS cells: nicotinamide adenine dinucleotide-malic enzyme (NAD-ME), nicotinamide adenine dinucleotide phosphate-malic enzyme (NADP-ME), and phosphoenolpyruvate carboxykinase (PEPCK). Although C_4 subtypes had initially been defined by these main decarboxylases (Hatch et al., 1975), more recent work suggests there is a greater degree of nuance than traditional C_4 classifications connote, as NADP-ME and NAD-ME often operate alongside a PEPCK auxiliary pathway, and the energetic requirements of C_4 photosynthesis render a pure PEPCK subtype unlikely (Wang et al., 2014a). Variations across C_4 species and phylogenetic distance are thus important considerations when trying to derive generic differences between C_3 and C_4 photosynthesis.

In this study we analysed steady state photosynthesis and photosynthetic induction in three phylogenetically linked pairs of C_3 and C_4 species from *Alloteropsis*, *Flaveria*, and *Cleome* genera, representative of monocots and dicots, and all three C_4 decarboxylation enzymes. Photosynthetic gas exchange was measured in response to a step-change to moderate and strongly saturating light intensities to characterise differences in photosynthetic induction rates. Experiments were conducted at both 21% and 2% O_2 concentration to evaluate the role of photorespiration during induction. Activation of CO_2 assimilation at the start of light induction was slower in all C_4 species compared to their C_3 counterparts although the mechanism of impairment varied across genera. Furthermore, although both C_3 and C_4 *Flaveria* had greater CO_2 assimilation under 2% O_2, assimilation in C_3 and C_4 *Alloteropsis* species as well as C_3 *T. hassleriana* was negatively impacted by low O_2. The variation in responses highlights the natural diversity of C_4 species, and the importance of controlling for phylogenetic distance in comparisons between C_3 and C_4 photosynthesis.

Materials and methods

Plant materials

Three pairs of phylogenetically linked *Alloteropsis*, *Flaveria* and *Cleome* C_3 and C_4 species were selected to decrease evolutionary variation within each pair (see Figure 1) (Lyu et al., 2015) but maintain significant evolutionary distance between the three genera, as C_4 origins arose ~ 17 million years ago (Ma) in *Cleome*, ~ 2 Ma in *Flaveria*, and even earlier in *Alloteropsis* (Christin et al., 2011; Lundgren et al., 2015). The selected species include monocots (C_3 *Alloteropsis semialata* subspecies *semialata* accession *GMT* and C_4 *Alloteropsis semialata* subspecies *eckloniana* accession *MDG*), dicots (C_3 *Flaveria cronquistii*, C_4 *Flaveria bidentis*, C_3 *Tarenaya hassleriana* and C_4 *Gynandropsis gynandra*), and the three major decarboxylase enzymes of the C_4 pathway, which have been suggested to be dominant in different C_4 species: PEPCK in mixed NADP-ME-PEPCK pathway in *A. semialata MDG* (Ueno and Sentoku, 2006), NADP-ME in *F. bidentis* (Gowik et al., 2011), and NAD-ME in *G. gynandra* (Bräutigam et al., 2010).

Plant growth and propagation

All plants were measured during the vegetative growth phase. Plants were grown in Levington Advance M3 compost (Scotts, Ipswich, UK) mixed with Miracle-Gro All Purpose Continuous Release Osmocote (Scotts Miracle-Gro Company, Marysville, OH, USA; 4 L compost: 25g Osmocote). Medium vermiculite was added to the *Alloteropsis* soil mix (4 L compost: 1 L vermiculite: 25g Osmocote) to prevent waterlogging.

The *Alloteropsis GMT* and *MDG* accessions were vegetatively propagated and grown on 2 L pots under well-watered conditions in a glasshouse at 18-25°C, 40-60% relative humidity (RH), with supplemental lightning provided to ensure at least 140-160 μmol m^{-2} s^{-1} photon flux density (PFD) across a

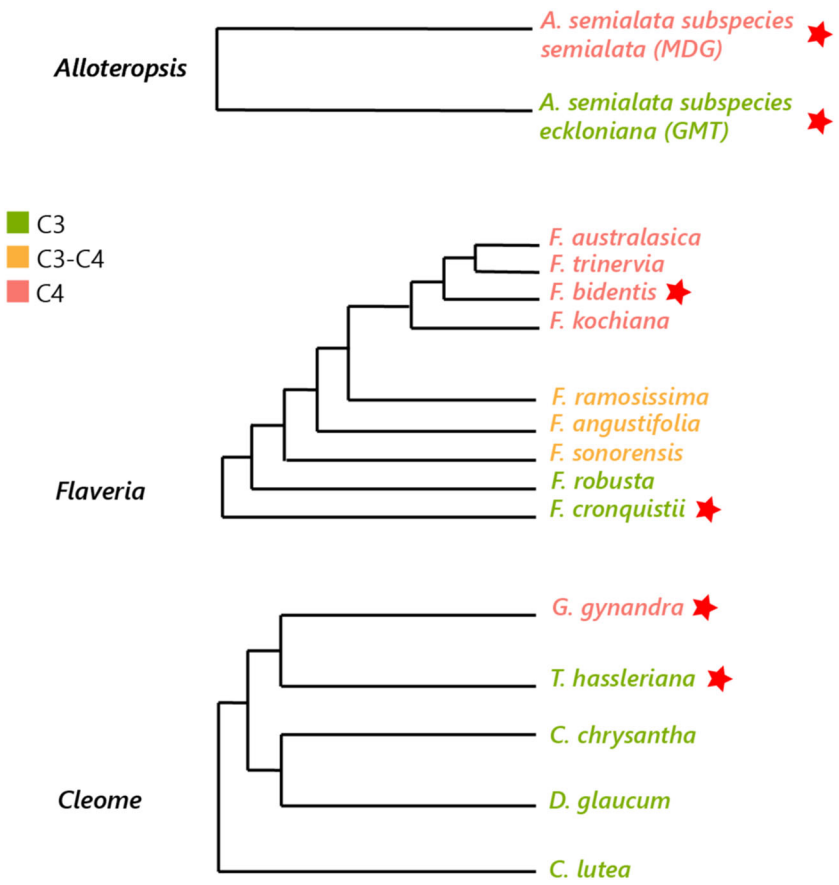

FIGURE 1
Phylogenetic tree of *Alloteropsis*, *Flaveria* and *Cleome* genera. Species used in the study are marked with a red star (adapted from Ibrahim et al., 2009; Lyu et al., 2015; Shi et al., 2021).

16-hour photoperiod. Plants were measured two weeks after propagation.

The *Flaveria* and *Cleome* species were grown under well-watered conditions in a Conviron growth room (Conviron Ltd., Winnipeg, MB, CA) at 20°C temperature, 60% RH, and 150 µmol m^{-2} s^{-1} PFD over a 16-hour photoperiod. Because *F. cronquistii* requires vegetative propagation, plants from both *Flaveria* species were propagated from lateral shoot cuttings – *F. bidentis* plants were initially grown from seed and then propagated. Cuttings were dipped in Doff Hormone Rooting Powder (Doff Portland Ltd., Hucknall, UK) to induce root development, and *Flaveria* cuttings were grown on 0.25 L pots and measured after 8-10 weeks.

Cleome germination was induced under sterile conditions at 30°C/20°C day/night cycle for *T. hassleriana*, and at 30°C for *G. gynandra*. Germinated seeds were initially sown in 24-cell seed trays before transfer to 0.25 L pots. As *G. gynandra* has a lower development rate than *T. hassleriana*, germination was staggered so both species could be measured at approximately the same developmental stage, after 8-10 weeks for *G. gynandra* and 4-6 weeks for *T. hassleriana*.

Gas exchange and chlorophyll fluorescence

Gas exchange and chlorophyll fluorescence were measured simultaneously using an open gas exchange system (LI-6400XT, LI-COR, Lincoln, NE, USA) with an integrated leaf chamber fluorometer (6400-40 LCF). Leaves were measured in a 2 cm^2 chamber at 25°C block temperature, 410 ppm sample CO_2 concentration, and 50-65% RH with flow of 300 µmol s^{-1}. Average leaf VPD was 1.1 ± 0.1 kPa at the start and 1.35 ± 0.1 kPa at the end of the light treatment. Actinic light was provided by the LCF and composed of 10% blue (470 nm) and 90% red light (630 nm).

The LCF used a 0.25 Hz modulated measuring light and a multiphase flash (Loriaux et al., 2013) to measure steady (F') and maximal (F_m') fluorescence to derive the quantum yield of

Photosystem II (ΦPSII) (Genty et al., 1989).

For experiments using 2% O_2, a pre-mixed 2% O_2 and 98% N_2 gas mixture was supplied to the LI-6400XT through the air inlet, using a mass flow controller (EL-FLOW, Bronkhorst High-tech BV, Ruurlo, NL) and an open T-junction to regulate constant surplus flow. Infrared Gas Analyzer (IRGA) calibration was adjusted to the O_2 gaseous composition in the instrument settings prior to measurement.

Leaf absorptance

Light absorptance of the plants used in experiments was measured with an integrating sphere (LI-1800-12, LI-COR) optically connected to a miniature spectrometer (Li-Cor, 1988). Incident PFD was converted to absorbed photon flux density (PFD_{abs}) using the measured leaf absorptance of the emission wavelengths of the 6400-40 LCF light source. The specific absorptance values can be found in Supplementary Material 1.

Steady state light response curves

Steady state light response curves of photosynthetic gas exchange were measured for all species at both 21% and 2% O_2. Leaves were light-adapted at 1000 μmol m^{-2} s^{-1} PFD and once CO_2 assimilation and stomatal conductance reached steady state, gas exchange and chlorophyll fluorescence parameters were measured in a descending gradient of light intensity: 2000, 1700, 1500, 1200, 1000, 800, 600, 400, 300, 200, 100, 75, 30, and 0 μmol m^{-2} s^{-1} PFD. Gas exchange and chlorophyll fluorescence parameters were logged after 120 – 240 s, when leaf intracellular CO_2 concentration (C_i) and CO_2 assimilation were stable.

To analyse steady state responses, a non-rectangular hyperbola was fitted to the light response curves (Stinziano et al., 2021). The quantum yield of assimilation (α) was derived from the initial slope, and the light-saturated photosynthetic rate (A_{max}) from the asymptote of the curve. C_i values obtained above 600 μmol m^{-2} s^{-1} PFD were averaged to estimate light-saturated C_i ($C_{i\ max}$).

Approximate light intensities at the inflection point (600 μmol m^{-2} s^{-1} PFD) and in the saturating part of the response (1500 μmol m^{-2} s^{-1} PFD) were used in the light induction experiments. Respiration in the light (*Rd*) was estimated for all species at each O_2 concentration as the y-intercept using a linear regression of the initial light response curve slope. To account for the Kok effect, measurements in darkness and at 30 μmol m^{-2} s^{-1} light intensity were not included in the regression (Kok, 1949).

Light induction experiments and analysis of lag in carbon assimilation

Leaves were dark-adapted until stomatal conductance reached constant levels (between 30-60 minutes depending on the species), illuminated with 600 μmol m^{-2} s^{-1} or 1500 μmol m^{-2} s^{-1} PFD for 1 hour, and then returned to darkness for another half hour. Starting from the last 5 minutes of initial dark adaption, gas exchange parameters were logged every minute, and chlorophyll fluorescence parameters at 5, 15, 25, 35, 45, and 60 minutes after starting light exposure. Light induction experiments at both light intensities were conducted at 21% and 2% O_2. Carbon assimilation was corrected for respiration to determine net photosynthetic CO_2 assimilation (A_{CO2}) using the *Rd* obtained from light response curves.

To analyse photosynthetic responses across the induction period, the trapezoidal rule (Jawień, 2014) was used to integrate the area under the curve (AUC) (Makowski et al., 2019) of A_{CO2} during the 0 – 5, 5 – 10, and 10 – 60 minute phases of light exposure.

Alternative electron sinks

The electron cost of assimilation can be approximated by the ΦPSII/ΦCO_2 ratio (Genty et al., 1989; Oberhuber and Edwards, 1993), with ΦCO_2 being the quantum yield of CO_2 assimilation (**Equation 1**). Lower ratios are associated with greater coupling as more electrons captured by PSII go towards CO_2 assimilation (Krall and Edwards, 1990). For light response curves the ΦPSII/ΦCO_2 ratio was calculated for the values obtained at 600 μmol m^{-2} s^{-1} PFD (*600* ΦPSII/ΦCO_2) and 1500 μmol m^{-2} s^{-1} PFD (*1500* ΦPSII/ΦCO_2). During light induction ΦPSII/ΦCO_2 values were taken from across the light period at each intensity. Data points were excluded if calculated ΦCO_2 showed negative values.

$$\Phi CO_2 = \frac{(A_{CO2} + Rd)}{PFD_{abs}} \qquad \text{Equation 1}$$

Statistical analysis

All statistical analyses were conducted separately on paired *Alloteropsis, Flaveria*, and *Cleome* light response curves, light induction at 600 μmol m^{-2} s^{-1} PFD, and light induction at 1500 μmol m^{-2} s^{-1} PFD. Mean and standard error of the mean of light response curve parameters (A_{max}, α, $C_{i\ max}$, *600* ΦPSII/ΦCO_2 and *1500* ΦPSII/ΦCO_2), A_{CO2} AUC at different phases of induction, and ΦPSII/ΦCO_2 across light induction were

calculated. Linear mixed models (LMMs) were fitted to the light response curve parameters and A_{CO2} AUC at different phases of induction using photosynthetic pathway, O_2 concentration and their interaction as fixed effects; and to ΦPSII/ΦCO_2 across light induction using photosynthetic pathway, O_2 concentration, time, and their interactions as fixed effects. Time of day and measured plant were included as random effects in all models. Two and three-way ANOVA tables for the fixed effects were generated from the LMMs using the Satterthwaite's approximation method (Kuznetsova et al., 2017). The data was independent and assumptions of normality, homogeneity of variance and sphericity were satisfied.

All data analysis and plot generation was done on RStudio 1.3 (RStudio Team, 2022) with R 4.1.1 (R Core Team, 2021) using the tidyverse (Wickham et al., 2019), RColorBrewer (Neuwirth, 2014), lme4 (Bates et al., 2015), lmerTest (Kuznetsova et al., 2017) and bayestestR libraries (Makowski et al., 2019).

Results

Steady state measurements confirm canonical differences in CO_2 assimilation between C_3 and C_4 species

Light response curves were used to first characterise C_3 and C_4 responses under steady state at 21% (Figures 2A-C, 3A-C and Table 1). The responses of C_4 species in comparison to their C_3 phylogenetic pairs were genus specific – C_4 *F. bidentis* had higher maximum rates of net carbon assimilation (A_{max}) than C_3 *F. cronquistii* ($P = 0.03$; C_3 12.5 ± 1.3 vs C_4 16.7 ± 1.0 μmol m^{-2} s^{-1}), but A_{max} values in C_4 *G. gynandra* were similar to those found in C_3 *T. hassleriana* ($P = 0.24$; C_3 15.5 ± 2.0 vs C_4 16.7 ± 0.7 μmol m^{-2} s^{-1}), and A_{max} values in C_4 *A. semialata MDG* also were similar to C_3 *A. semialata GMT* ($P = 0.02$; C_3 11.8 ± 1.1 vs C_4 10.2 ± 2.7 μmol m^{-2} s^{-1}). A two-way ANOVA (Table 2) showed photosynthetic pathway had a significant effect on C_i during light saturation in all genera. However, whilst the C_4 pathway was associated with lower $C_{i\ max}$ in *Flaveria* ($P \leq 0.001$; C_3 238 ± 19 vs C_4 86 ± 27 μmol mol^{-1}) and *Cleome* ($P \leq 0.001$; C_3 310 ± 8 vs C_4 125 ± 27 μmol mol^{-1}), in *Alloteropsis* the C_4 association was instead with higher $C_{i\ max}$ ($P \leq 0.01$; C_3 242 ± 9 vs C_4 285 ± 21 μmol mol^{-1}). Figure 2C shows that the lower C_i of C_4 species corresponded to lower stomatal conductance, excepting C_4 *A. semialata MDG*, where stomatal conductance to water vapour (g_{sw}) was similar to C_3 *A. semialata GMT* across the light response.

ΦPSII decreased exponentially with higher light intensities. Although ΦPSII values were very similar across C_3 and C_4 pairs in *Flaveria* and *Cleome*, more pronounced decreases were observed in C_4 *A. semialata MDG* than in C_3 *A. semialata GMT* (Figure 3A). ΦCO_2 was also lower at higher light intensities, following a similar pattern to A_{max} across the light response, as ΦCO_2 was similar between C_3 and C_4 species in *Alloteropsis* and *Cleome*, but higher in C_4 *F. bidentis* compared to C_3 *F. cronquistii* (Figure 3B). These differences across genera were also apparent for the observed ΦPSII and ΦCO_2 ratios, but not always significantly so. C_4 *F. bidentis* had lower ΦPSII/ΦCO_2 than C_3 *F. cronquistii* ($P = 0.16$; C_3 14.0 ± 0.3 vs C_4 9.0 ± 2.4 at PFD = 600 μmol m^{-2} s^{-1}, and $P = 0.56$; C_3 12.2 ± 0.6,

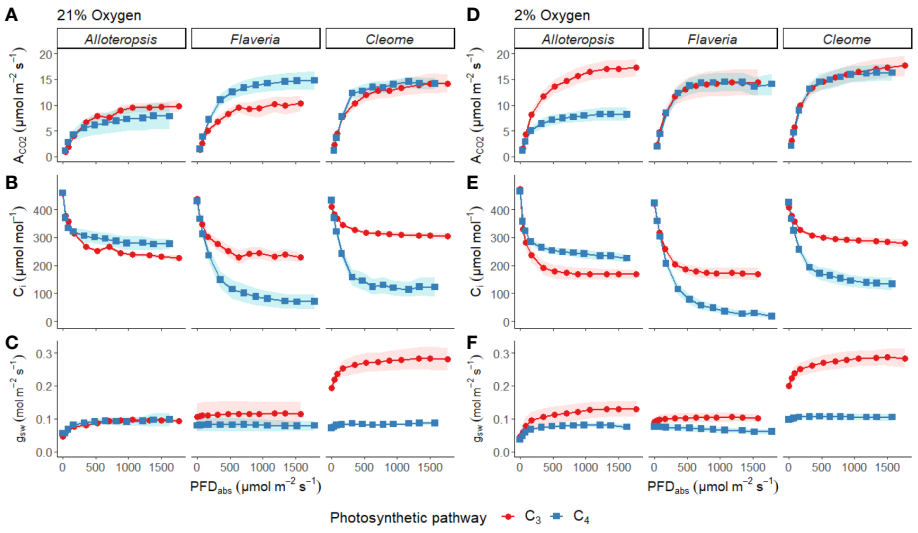

FIGURE 2
Measurements of gas exchange traits during light response curves for phylogenetically linked C_3 and C_4 *Alloteropsis*, *Flaveria* and *Cleome* species under 21% and 2% O_2. Plots show net CO_2 assimilation (A_{CO2}, **A, D**), intercellular CO_2 concentration (C_i, **B, E**), and stomatal conductance to water vapour (g_{sw}, **C, F**) as a function of absorbed light intensity. Ribbons represent standard error of the mean (n=5).

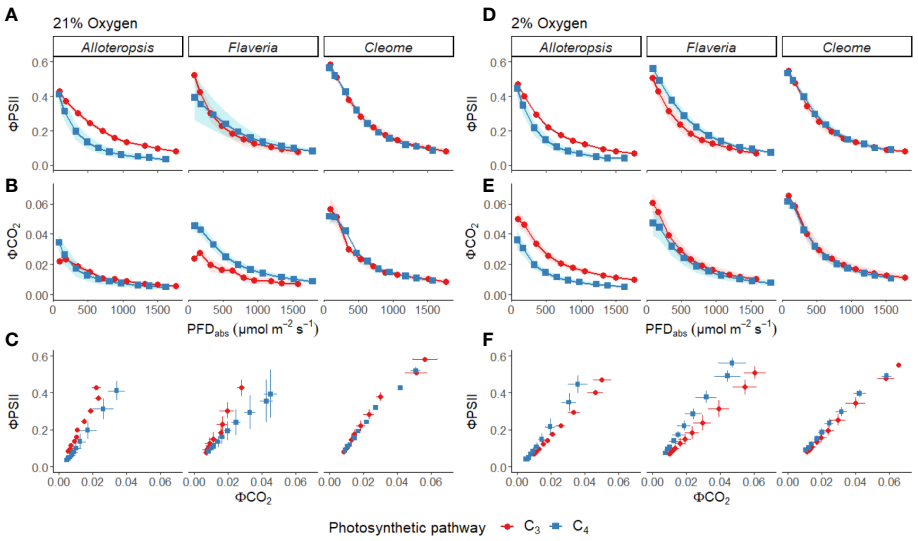

FIGURE 3
Measurements of gas exchange and chlorophyll fluorescence traits during light response curves for phylogenetically linked C_3 and C_4 *Alloteropsis*, *Flaveria* and *Cleome* species under 21% and 2% O_2. Plots show quantum yield of PSII (ΦPSII, **A**, **D**), and quantum yield of CO_2 assimilation (ΦCO_2, **B, E**) as a function of absorbed light intensity. Ribbons represent standard error of the mean (n=5). Plots **(C, F)** display the relationship between ΦPSII and ΦCO_2. Error bars represent standard error of the mean for both parameters.

C_4 9.5 ± 2.2 at PFD = 1500 μmol m^{-2} s^{-1}) and the same was observed for C_4 *A. semialata MDG* compared to C_3 *A. semialata GMT* (P = 0.03; C_3 16.7 ± 1.8 vs C_4 11.3 ± 2.4 at PFD = 600 μmol m^{-2} s^{-1}, and $P \leq 0.001$; C_3 16.2 ± 1.6 vs C_4 8.6 ± 2.1 at PFD = 1500 μmol m^{-2} s^{-1}), suggesting that in these C_4 species less electron transfer through PSII is needed per CO_2 fixed. Figure 3C shows that the lower ratio of ΦPSII to ΦCO_2 in C_4 *Flaveria* and *Alloteropsis* in relation to their C_3 counterparts was observed across most light intensities, although the difference appeared to be marginal at higher light intensities. At 21% O_2, both C_3 and C_4 *Cleome* species had very similar ΦPSII/ΦCO_2 (P = 0.84; C_3 12.3 ± 0.8 vs C_4 11.7 ± 1.1 at PFD = 600 μmol m^{-2} s^{-1}, and P = 0.78; C_3 10.5 ± 0.5 vs C_4 9.8 ± 1.0 at PFD = 1500 μmol m^{-2} s^{-1}).

Light response curves were also performed at 2% O_2 to minimize photorespiration (Figures 2D-F, 3D-F and Table 1). All three C_3 species had substantially higher CO_2 assimilation rates under low O_2 – A_{max} was around 75% higher in C_3 *A. semialata MDG*, 25% higher in C_3 *F. cronquistii*, and 35% higher in C_3 *T. hassleriana* than under 21% O_2. 2% O_2 also led to a decrease in $C_{i\ max}$ in *Alloteropsis* ($P \leq 0.01$ in C_3 171 ± 19 vs C_4 240 ± 14 μmol mol^{-1}) and *Flaveria* (P = 0.02; C_3 174 ± 18 vs C_4 43 ± 15 μmol mol^{-1}) but no significant change in either *Cleome* species (P = 0.93; C_3 290 ± 11 vs C_4 149 ± 21 μmol mol^{-1}), where A_{CO2} and g_{sw} appeared tightly coordinated. The increase in A_{max} was not mirrored in C_4 species, as evidenced by significant interactions (Table 2) between photosynthetic pathway and oxygen in *Alloteropsis* (P = 0.03) and *Flaveria* (P = 0.01), where low O_2 concentrations were associated with higher A_{max} on C_3 but not C_4 species. (Table 2). Similar patterns were observed for the two *Cleome* species, however the increase in A_{max} at 2% O_2 for C_3 *T. hassleriana* was less pronounced than for the other C_3 species and instead the initial slope α appeared to be subject to a significant interaction between effects of photosynthetic pathway and O_2 (P = 0.03). The different effects on assimilation at low O_2 between C_3 and C_4 species were also reflected in the changing relationship between ΦPSII and ΦCO_2 (Figures 3C, F) – photosynthetic pathway and O_2 concentration were found to have significant interactions on ΦPSII/ΦCO_2 in all three genera (Table 2, P = 0.05 in *Flaveria* and *Cleome*, $P \leq 0.01$ in *Alloteropsis*), due to decreases in ΦPSII/ΦCO_2 in C_3 species at 2% O_2 not observed in C_4 species. This data confirms that photorespiration is a significant electron sink under steady state for all three C_3 species, whereas the steady state suppression of photorespiration at 21% O_2 in the C_4 species is sufficient to prevent any significant further decreases in ΦPSII/ΦCO_2 under 2% O_2.

Substantial differences in photosynthetic traits exist between C_3 and C_4 species during light induction

Photosynthetic induction rates were measured in leaves exposed to 600 μmol m^{-2} s^{-1} or 1500 μmol m^{-2} s^{-1} PFD from darkness (Figures 4A-C, G-I). The light induction response across

TABLE 1 Light response curve parameters estimated from steady state light response curves under 21% and 2% O_2 on phylogenetically linked C_3 and C_4 *Alloteropsis*, *Flaveria* and *Cleome* species.

		21% Oxygen		2% Oxygen	
Genus	Parameter	C_3	C_4	C_3	C_4
Alloteropsis	A_{max} (μmol m^{-2} s^{-1})	11.8 ± 1.1	10.2 ± 2.7	20.9 ± 2.4	10.3 ± 1.4
	α	0.04 ± 0.00	0.10 ± 0.02	0.08 ± 0.01	0.09 ± 0.01
	$C_{i\ max}$ (μmol mol^{-1})	242 ± 9	285 ± 21	171 ± 19	240 ± 14
	600 ΦPSII/ΦCO_2	16.7 ± 1.8	11.3 ± 2.4	8.9 ± 1.7	10.0 ± 2.4
	1500 ΦPSII/ΦCO_2	16.2 ± 1.6	8.6 ± 2.1	7.5 ± 1.2	6.8 ± 2.6
	Rd	0.9 ± 0.2	1.4 ± 0.6	1.5 ± 0.3	1.5 ± 0.1
Flaveria	A_{max} (μmol m^{-2} s^{-1})	12.5 ± 1.3	16.7 ± 1.0	15.6 ± 1.7	15.3 ± 1.8
	α	0.07 ± 0.02	0.06 ± 0.01	0.07 ± 0.01	0.06 ± 0.01
	$C_{i\ max}$ (μmol mol^{-1})	238 ± 19	86 ± 27	174 ± 18	43 ± 15
	600 ΦPSII/ΦCO_2	14.0 ± 0.3	9.0 ± 5.2	7.6 ± 0.3	12.6 ± 3.2
	1500 ΦPSII/ΦCO_2	12.2 ± 0.6	9.5 ± 2.2	8.1 ± 0.6	11.1 ± 3.2
	Rd	0.9 ± 0.3	1.0 ± 0.4	0.6 ± 0.2	0.4 ± 0.2
Cleome	A_{max}	15.5 ± 2.0	16.7 ± 0.7	20.9 ± 2.5	17.7 ± 1.5
	α	0.07 ± 0.01	0.09 ± 0.02	0.15 ± 0.03	0.08 ± 0.01
	$C_{i\ max}$ (μmol mol^{-1})	310 ± 8	125 ± 27	290 ± 11	149 ± 21
	600 ΦPSII/ΦCO_2	12.3 ± 0.8	11.7 ± 1.1	7.7 ± 1.0	9.4 ± 0.5
	1500 ΦPSII/ΦCO_2	10.5 ± 0.5	9.8 ± 1.0	8.7 ± 0.7	8.8 ± 0.3
	Rd	0.3 ± 0.2	1.8 ± 0.7	2.1 ± 0.7	0.8 ± 0.5

The light-saturated photosynthetic rate (A_{max}) and the quantum yield of assimilation (α) were calculated by fitting the light response curves with a non-rectangular hyperbola. The C_i at light saturation point ($C_{i\ max}$) is the average C_i at PFD ≥ 600 μmol m^{-2} s^{-1}. Values for *600* ΦPSII/ΦCO_2 and *1500* ΦPSII/ΦCO_2 were taken at PFD = 600 μmol m^{-2} s^{-1} and PFD =1500 μmol m^{-2} s^{-1}. Means and standard error of the mean are shown (n = 5).

all species and light intensities generally consisted of gradual stomatal opening in line with a rise in A_{CO2} towards steady state, and a sharp drop in C_i at the start of induction, followed by a gradual recovery.

In addition to these general patterns, several differences were observed across genera and between paired species. Stomata tended to open more quickly in the C_3 species than in their respective C_4 counterparts. Furthermore, the speed of A_{CO2} induction appeared to vary between some C_3 and C_4 pairs; where carbon assimilation was notably slower to induce in C_4 *G. gynandra* compared to C_3 *T. hassleriana* under both light intensities, with more subtle differences observed in the *Alloteropsis* and *Flaveria* C_3 and C_4 pairs.

Reductions in assimilation of CO_2 at the start of induction in C_3 and C_4 species vary across genera

In order to systematically explore C_3 and C_4 differences in the activation of CO_2 assimilation, the induction time-series were subdivided into three periods, 0 – 5 min, 5 – 10 min, and the remaining 10 – 60 min, and integrated carbon assimilation (AUC) was calculated for each period (Figure 5). During the 0 – 5 min period, C_4 *F. bidentis* had lower AUC than C_3 *F. cronquistii* under both PFD = 600 μmol m^{-2} s^{-1} ($P = 0.09$; C_3 12.4 ± 1.7 vs C_4 5.8 ± 2.0 μmol m^{-2}) and PFD = 1500 μmol m^{-2} s^{-1} ($P = 0.02$; C_3 14.8 ± 1.8 vs C_4 8.0 ± 1.8 μmol m^{-2}), with the difference becoming significant under higher light (Table 3). The difference in assimilated CO_2 between C_3 and C_4 species at the start of induction was even more pronounced in *Cleome*, where the AUC of C_4 *G. gynandra* was significantly lower than that of C_3 *T. hassleriana* under both light intensities ($P \leq 0.01$; C_3 12.6 ± 2.0 vs C_4 -1.4 ± 1.9 μmol m^{-2} at PFD = 600 μmol m^{-2} s^{-1}, and $P \leq 0.01$; C_3 13.8 ± 3.2 vs C_4 -3.1 ± 1.8 μmol m^{-2} at PFD = 1500 μmol m^{-2} s^{-1}). The AUC in C_4 *G. gynandra* continued to be significantly lower than in C_3 *T. hassleriana* under both light intensities during the following two periods of induction analysed (Table 3). In contrast, the significant difference in cumulative CO_2 uptake between *Flaveria* species was only significant during the first five minutes of induction (Figure 5A). Thus, there was a more pronounced lag in CO_2 assimilation during induction in C_4 photosynthesis in *Flaveria* and *Cleome* than in C_3 photosynthesis in the same genera. This was

10.3389/fpls.2022.1091115

TABLE 2 ANOVA table of modelled light response curve parameters for phylogenetically linked C_3 and C_4 *Alloteropsis*, *Flaveria* and *Cleome* species.

		Alloteropsis			*Flaveria*			*Cleome*		
Parameter		PP	$[O_2]$	PP:$[O_2]$	PP	$[O_2]$	PP:$[O_2]$	PP	$[O_2]$	PP:$[O_2]$
A_{max}	df; *F*-value; *P*-value	1,15; 7.40; **0.02**	1,15; 4.47; 0.06	1,15; 5.90; **0.03**	1,15; 5.81; **0.03**	1,15; 1.40; 0.26	1,15; 7.73; **0.01**	1,15; 0.29; 0.59	1,15; 3.19; 0.09	1,15; 1.51; 0.24
α	df; *F*-value; *P*-value	1,15; 3.89; 0.06	1,15; 1.85; 0.20	1,15; 3.69; 0.07	1,15; 1.38; 0.26	1,15; 0.03; 0.87	1,15; 0.26; 0.62	1,15; 1.45; 0.24	1,15; 3.77; 0.07	1,15; 5.58; **0.03**
C_{imax}	df; *F*-value; *P*-value	1, 16; 11.06; **≤0.01**	1, 16; 12.00; **≤0.01**	1, 16; 0.54; 0.45	1, 16; 49.07; **≤0.001**	1, 16; 6.75; **0.02**	1, 16; 0.27; 0.61	1, 16; 70.23; **≤0.001**	1, 16; 0.00; 0.93	1, 16; 1.27; 0.27
600 ΦPSII/$ΦCO_2$	df; *F*-value; *P*-value	1,16; 6.05; **0.03**	1,16; 24.29; **≤0.001**	1,16; 12.28; **≤0.01**	1,16; 2.01; 0.16	1,16; 5.31; **0.05**	1,16; 5.95; **0.03**	1,16; 0.05; 0.84	1,16; 30.01; **≤0.01**	1,16; 5.39; **0.05**
1500 ΦPSII/ $ΦCO_2$	df; *F*-value; *P*-value	1,16; 22.75; **≤0.001**	1,16; 35.56; **≤0.001**	1,16; 15.67; **≤0.01**	1,16; 0.37; 0.56	1,16; 1.55; 0.26	1,16; 6.68; **0.05**	1,16; 0.08; 0.78	1,16; 15.61; **0.01**	1,16; 5.57; **0.05**

Photosynthetic pathway, PP. O_2 concentration, $[O_2]$. Interaction effect, PP:$[O_2]$. Table shows degrees of freedom; *F*-value; and *P*-value. Significant (a< 0.05) *P*-values are shown in bold.

especially apparent in relation to the steady state comparison between both species-pairs (Figure 2A). In *Alloteropsis*, the C_4 *A. semialata MDG* also started at lower AUC than C_3 *A. semialata GMT* during the 0 – 5 min period under both light intensities (P = 0.36; C_3 -4.4 ± 0.5 vs C_4 -6.22 ± 0.39 at PFD = 600 µmol m^{-2} s^{-1}, and P = 0.07; C_3 -4.2 ± 0.2, vs C_4 -6.8 ± 0.6 at PFD = 1500 µmol m^{-2} s^{-1}), but the difference in AUC between pathways was only found to be significant for the final 10 – 60 min ($P \leq 0.01$; C_3 194.8 ± 34.3 vs C_4 142.2 ± 101.0 at PFD = 600 µmol m^{-2} s^{-1}, and P = 0.03; C_3 403.3 ± 59.5 vs C_4 241.5 ± 115.6 at PFD = 1500 µmol m^{-2} s^{-1}).

CO_2 assimilation during induction is enhanced under 2% O_2 in some species but suppressed in others

In order to test whether the presence or absence of photorespiration affected the activation of CO_2 assimilation, both light treatments were also conducted under 2% O_2 (Figures 4D-F, J-L). In *Flaveria*, the decrease in O_2 concentration significantly increased the AUC of both C_3 *F. cronquistii* and C_4 *F. bidentis* during the first five minutes of induction (Table 3 and Figure 5A), under both light intensities ($P \leq 0.01$; C_3 26.1 ± 5.4 vs C_4 19.9 ± 2.6 µmol m^{-2} at PFD = 600 µmol m^{-2} s^{-1} and $P \leq 0.001$; C_3 33.8 ± 6.3 vs C_4 23.1 ± 1.6 at PFD = 1500 µmol m^{-2} s^{-1}). Interestingly, although the stimulating effect of 2% O_2 on C_4 *F. bidentis* was less pronounced for 5 – 10 min and 10 – 60 min, the effect was still significant across both periods under both light intensities, except for 5 – 10 min at PFD = 600 µmol m^{-2} s^{-1} (P = 0.08, Table 3). This suggests that photorespiration is insufficiently suppressed during induction in C_4 *F. bidentis*, whereas in contrast, no change was observed for CO_2 assimilation in steady state C_4 *F. bidentis* under 2% O_2 (Figures 2A, D). In *Cleome* no such enhancement of the photosynthetic response was observed in C_4 *G. gynandra*. Instead, the significant interaction between photosynthetic pathway and O_2 concentration from 0 – 5 min was primarily associated with a decrease in assimilated CO_2 in C_3 *T. hassleriana* and only a marginal increase in C_4 *G. gynandra* AUC under 2% O_2 compared to under 21% O_2 ($P \leq 0.001$). The negative effect of 2% O_2 on AUC in C_3 *T. hassleriana* was transiently observed from 0 – 10 min at PFD = 600 µmol m^{-2} s^{-1} and only from 0 – 5 min at PFD = 1500 µmol m^{-2} s^{-1}. From 10 – 60 min AUC at 2% O_2 in C_3 *T. hassleriana* was similar to the AUC at 21% O_2 under both light intensities. Thus, the stimulation of steady state CO_2 assimilation by 2% O_2 in this species was not observed under any of the transient conditions (Table 3 and Figure 5). Suppression of carbon assimilation by low O_2 was also observed during the start of induction in both C_3 and C_4 *Alloteropsis* species. The AUC from 0 – 5 min was reduced in C_3 *A. semialata GMT* and C_4 *A. semialata MDG* compared to AUC in 21% O_2 under both light intensities, a significant effect ($P \leq 0.001$) that persisted well into the 5 – 10 min period for PPFD = 600 µmol m^{-2} s^{-1} ($P \leq 0.02$). However, by 10 – 60 min the effect of O_2 was reversed in C_3 *A. semialata GMT*, with AUC for this period being significantly higher than for 21% O_2 (P = 0.03). For this period C_3 *A. semialata GMT* also had a significantly higher AUC in 2% O_2 than C_4 *A. semialata MDG* ($P \leq 0.01$; C_3 504.4 ± 57.5 vs C_4 116.4 ± 84.7 µmol m^{-2} at PFD = 600 µmol m^{-2} s^{-1}, and P = 0.03; C_3 558.71 ± 94.6 vs C_4 285.2 ± 108.7 µmol m^{-2} at PFD

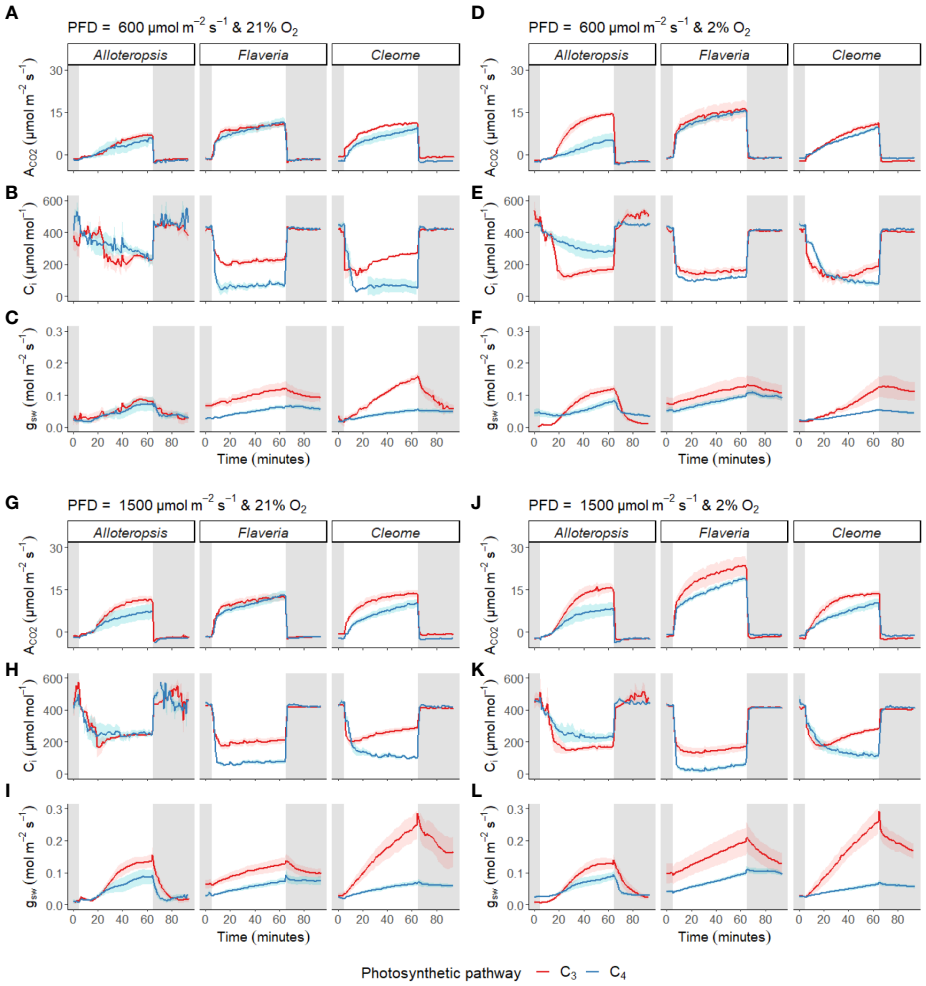

FIGURE 4
Measurements of gas exchange during light induction in phylogenetically linked C_3 and C_4 *Alloteropsis*, *Flaveria* and *Cleome* species. Leaves were acclimated to darkness, exposed to 1 hour of light, and returned to darkness for another half hour. Plots show net CO_2 assimilation (A_{CO2}, **A, D, G, J**), intercellular CO_2 concentration (C_i, **B, E, H, K**) and stomatal conductance to water vapour (g_{sw}, **C, F, I, L**) across the light induction experiment, at PFD = 600 µmol m^{-2} s^{-1} and PFD = 1500 µmol m^{-2} s^{-1}, in 21% and 2% O_2. Ribbons represent standard error of the mean (n = 5).

= 1500 µmol m^{-2} s^{-1}). Whereas the stimulating effect of 2% O_2 on transient CO_2 assimilation may be indicative of photorespiration as a negative factor during photosynthetic induction, the suppression of carbon assimilation found under 2% O_2 for both *Alloteropsis* species as well as the *Cleome* C_3 *T. hassleriana* could indicate photorespiration is not always detrimental to photosynthetic efficiency and may indeed support the activation of CO_2 assimilation in some C_3 and C_4 species.

Transient decoupling between electron transport and carbon fixation during induction is more pronounced in C_4 species and ameliorated by 2% O_2

During activation of CO_2 assimilation, a temporary decoupling between the electron transport chain and photosynthetic carbon fixation in C_4 species could occur due to the time needed to activate the C_3 cycle, incomplete suppression of photorespiration due to an inactive CCM, or because of an increase in the energetic cost of carbon fixation *via* BS CO_2 leakage. To look for evidence of transient decoupling during induction, ΦPSII/ΦCO_2 ratios across the light induction period under each light and O_2 condition were further analysed within each genus (Figure 6 and Table 4).

The effect of time was significant for all genera. All the C_4 species showed higher ΦPSII/ΦCO_2 at the start of induction under 21% O_2, with values gradually decreasing as the leaves became more acclimated to the light conditions. The average ΦPSII/ΦCO_2 ratio during induction was also noticeably higher than the steady state ΦPSII/ΦCO_2 for all species, which ranged between 8-12 e^-/CO_2 depending on the species, indicating a

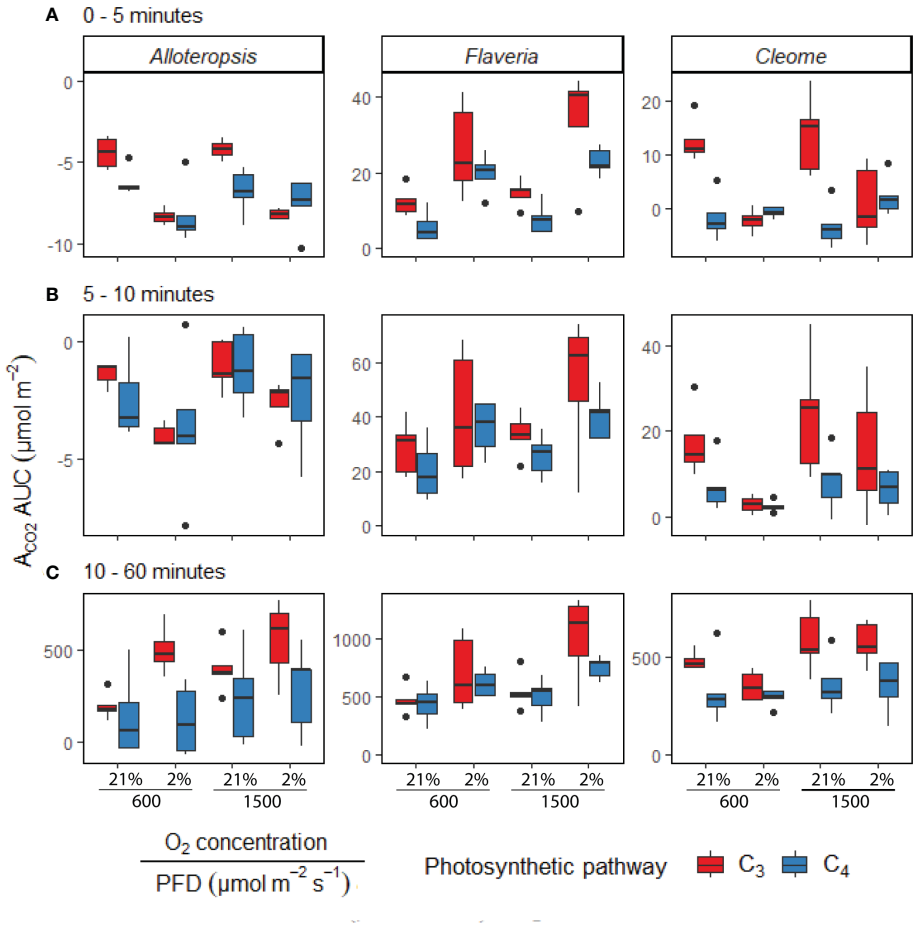

FIGURE 5
Boxplots of cumulative CO_2 assimilation over different phases of light induction in phylogenetically linked C_3 and C_4 *Alloteropsis*, *Flaveria* and *Cleome* species, under different light and O_2 treatments (n = 5 for each combination of species/measurement condition). Box edges represent first and third quartiles, the solid line indicates the median, and points represent outliers beyond 1.5 times the interquartile range. The area under the curve (AUC) was calculated from the A_{CO2} of light induction experiments where plants at 21% or 2% O_2 concentrations were dark-adapted and exposed to PFD = 600 µmol m^{-2} s^{-1} or PFD = 1500 µmol m^{-2} s^{-1} for 1 hour. Plots show the AUC of induction during 0 – 5 minutes **(A)**, 5 – 10 minutes **(B)**, and 10 – 60 minutes **(C)**. Two-way ANOVAs (Table 3) were used to test the effect of photosynthetic pathway, O_2 concentration and their interaction on A_{CO2} AUC at different phases of light induction in *Alloteropsis, Flaveria*, and *Cleome*.

significant transient decoupling during induction compared to steady state. In *Flaveria*, C_4 *F. bidentis* had higher ΦPSII/ΦCO_2 ratio than C_3 *F. cronquistii* under all light and oxygen conditions, the complete opposite of steady state. This suggests the C_4 pathway in *Flaveria* does have some features that make the activation of photosynthesis more energetically demanding at the onset of light induction. Notably, the interaction of O_2 concentration and time also had a significant effect on ΦPSII/ΦCO_2 ($P = 0.01$ at PFD = 600 µmol m^{-2} s^{-1}, $P = 0.01$ at PFD = 1500 µmol m^{-2} s^{-1}), since in 2% O_2 the ratio decreased at an earlier point of induction than in 21% O_2. During induction at PFD = 600 µmol m^{-2} s^{-1}, the three-way interaction was significant ($P = 0.04$), reflecting the strong decrease in ΦPSII/ΦCO_2 over time observed at 21% O_2 in C_4 *F. bidentis*. This decrease may reflect the progressive suppression of photorespiration by activation of the C_4 CCM, since the same trend in ΦPSII/ΦCO_2 was not present in C_3 *F. cronquistii*, nor under 2% O_2 when photorespiration would have been negligible.

In *Cleome*, C_3 *T. hassleriana* also had a lower ΦPSII/ΦCO_2 ratio than C_4 *G. gynandra*, in another reversal of differences observed during steady state conditions. ΦPSII/ΦCO_2 was significantly affected by time ($P \leq 0.01$ at PFD = 600 µmol m^{-2} s^{-1}, $P = 0.01$ at PFD = 1500 µmol m^{-2} s^{-1}) as well as O_2 concentration ($P \leq 0.001$ at both light intensities), but in contrast to *Flaveria* no significant interaction was found between O_2 and time ($P = 0.21$ at PFD = 600 µmol m^{-2} s^{-1}, $P = 0.47$ at PFD = 1500 µmol m^{-2} s^{-1}). Instead, in *Cleome* ΦPSII/ΦCO_2 was marginally lower at 2% O_2 than at 21% O_2 across the

TABLE 3 ANOVA table of the carbon assimilation AUC of different phases of light induction for phylogenetically linked C_3 and C_4 *Alloteropsis*, *Flaveria* and *Cleome* species.

			Alloteropsis			*Flaveria*			*Cleome*		
Light intensity (μmol m^{-2} s^{-1})	Induction phase (minutes)		PP	$[O_2]$	PP:$[O_2]$	PP	$[O_2]$	PP:$[O_2]$	PP	$[O_2]$	PP:$[O_2]$
600	0 – 5	df; *F*-value; *P*-value	1,16; 1.34; 0.26	1,16; 27.85; **≤0.001**	1,16; 3.13; 0.10	1,16; 3.18; 0.09	1,16; 15.08; **≤0.01**	1,16; 0.00; 0.95	1,16; 15.56; **≤0.01**	1,16; 15.12; **≤0.01**	1,16; 25.03; **≤0.001**
	5 – 10	df; *F*-value; *P*-value	1,16; 0.20; 0.66	1,16; 5.81; **0.02**	1,16; 0.80; 0.38	1,16; 0.86; 0.36	1,16; 3.60; 0.08	1,16; 0.05; 0.83	1,16; 5.01; **0.04**	1,16; 10.06; **≤0.01**	1,16; 2.95; 0.11
	10 – 60	df; *F*-value; *P*-value	1,16; 8.87; **≤0.01**	1,16; 3.68; 0.07	1,16; 5.14; **0.03**	1,16; 0.39; 0.54	1,16; 4.46; **0.05**	1,16; 0.08; 0.78	1,16; 4.58; **0.05**	1,16; 2.41; 0.14	1,16; 0.89; 0.36
1500	0 – 5	df; *F*-value; *P*-value	1,16; 3.81; 0.07	1,16; 22.30; **≤0.001**	1,16; 10.14; **≤0.01**	1,16; 6.39; **0.02**	1,16; 24.21; **≤0.001**	1,16; 0.33; 0.57	1,16; 9.48; **≤0.01**	1,16; 2.07; 0.17	1,16; 12.85; **≤0.01**
	5 – 10	df; *F*-value; *P*-value	1,16; 0.00; 0.99	1,16; 3.40; 0.08	1,16; 0.07; 0.78	1,16; 2.54; 0.13	1,16; 7.06; **0.01**	1,16; 0.12; 0.73	1,16; 5.90; **0.02**	1,16; 1.18; 0.29	1,16; 0.49; 0.49
	10 – 60	df; *F*-value; *P*-value	1,16; 5.09; **0.03**	1,16; 1.06; 0.31	1,16; 0.33; 0.57	1,16; 2.16; 0.16	1,16; 12.59; **≤0.01**	1,16; 1.01; 0.33	1,16; 12.96; **≤0.01**	1,16; 0.03; 0.86	1,16; 0.00; 0.95

Photosynthetic pathway, PP. O_2 concentration, $[O_2]$. Interaction effect, PP:$[O_2]$. Table shows degrees of freedom, *F*-value, and *P*-value. Significant (a< 0.05) *P*-values are shown in bold.

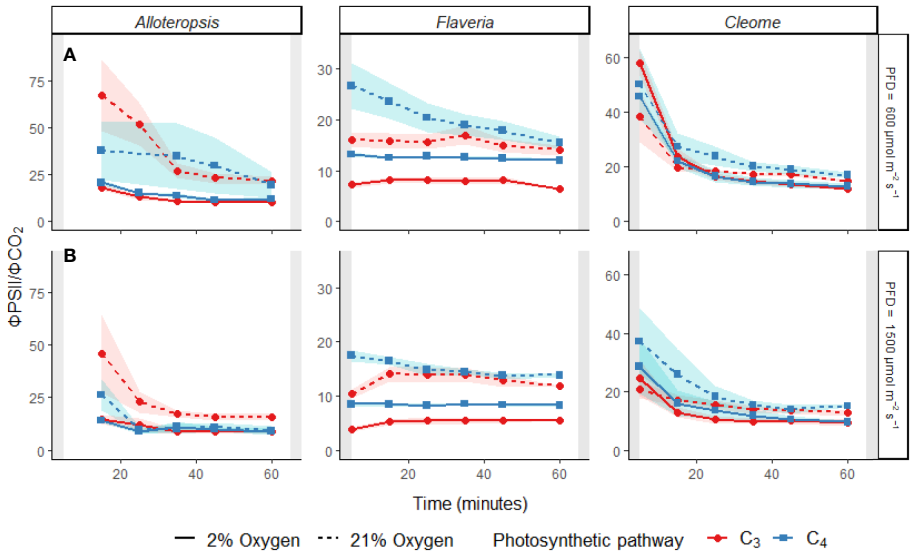

FIGURE 6
Line plots of the ΦPSII/$ΦCO_2$ ratio during light induction at PFD = 600 μmol m^{-2} s^{-1} **(A)** and PFD = 1500 μmol m^{-2} s^{-1} **(B)** in phylogenetically linked C_3 and C_4 *Alloteropsis*, *Flaveria* and *Cleome* species. Plots show ΦPSII/$ΦCO_2$ under 21% (dashed line) and 2% O_2 (solid line). Values of ΦPSII/$ΦCO_2$ were excluded if $ΦCO_2$ values were negative, resulting in the 5 minute *Alloteropsis* values being excluded. Ribbons show standard error of the mean (n = 5).

10.3389/fpls.2022.1091115

TABLE 4 ANOVA table of the ΦPSII/ΦCO_2 ratio during light induction for phylogenetically linked C_3 and C_4 *Alloteropsis*, *Flaveria* and *Cleome* species.

Light intensity (μmol m^{-2} s^{-1})	Genus		PP	t	$[O_2]$	PP:$[O_2]$	PP:t	O_2:t	PP:$[O_2]$: t
600	*Alloteropsis*	df; *F*-value; *P*-value	1,63; 0.11; 0.74	1,63; 28.69; **≤0.001**	1,63; 13.07; **≤0.001**	1,63; 0.71; 0.40	1,63; 0.62; 0.43	1,63; 5.98; **0.02**	1,63; 0.93; 0.34
	Flaveria	df; *F*-value; *P*-value	1,100; 52.64; **≤0.001**	1,100; 146.83; **≤0.001**	1,100; 6.96; **≤0.01**	1,100; 0.13; 0.73	1,100; 4.23; **0.04**	1,100; 6.60; **0.01**	1,100; 4.43; **0.04**
	Cleome	df; *F*-value; *P*-value	1,98; 0.69; 0.41	1,98; 7.71; **≤0.01**	1,98; 53.53; **≤0.001**	1,98; 1.57; 0.21	1,98; 0.00; 0.95	1,98; 0.04; 0.83	1,98; 0.30; 0.58
1500	*Alloteropsis*	df; *F*-value; *P*-value	1,70; 3.30; 0.07	1,70; 11.82; **≤0.001**	1,70; 12.50; **≤0.001**	1,70; 3.90; **0.05**	1,70; 0.60; 0.44	1,70; 4.20; **0.04**	1,70; 0.46; 0.49
	Flaveria	df; *F*-value; *P*-value	1,101; 67.884; **≤0.001**	1,101; 478.57; **≤0.001**	1,101; 0.60; 0.44	1,101; 2.06; 0.15	1,101; 9.33; **≤0.01**	1,101; 4.51; **0.03**	1,101; 2.91; 0.09
	Cleome	df; *F*-value; *P*-value	1,101; 4.14; **0.04**	1,101; 6.44; **0.01**	1,101; 27.65; **≤0.001**	1,101; 0.52; 0.47	1,101; 3.06; 0.08	1,101; 00.00; 0.96	1,101; 0.64; 0.42

Photosynthetic pathway, PP. Time, t. O_2 concentration, $[O_2]$. Interaction effects, PP:$[O_2]$, PP:t, and PP:$[O_2]$:t. Table shows degrees of freedom, *F*-value, and *P*-value. Significant (a< 0.05) *P*-values are shown in bold.

induction period. The temporal decrease in ΦPSII/ΦCO_2 was similar under both O_2 concentrations, suggesting that the transient decoupling between electron transport and CO_2 fixation was relatively insensitive to O_2 in both *Cleome* species.

Finally, ΦPSII/ΦCO_2 ratios in *Alloteropsis* were not significantly affected by a main effect of photosynthetic pathway (P = 0.74 at PFD = 600 μmol m^{-2} s^{-1}, P = 0.07 at PFD = 1500 μmol m^{-2} s^{-1}), again in contrast to steady state where C_4 *A. semialata MDG* had lower ratios than C_3 *A. semialata GMT*. However, the interaction between photosynthetic pathway and O_2 was significant ($P \leq 0.001$ at both light intensities), due to the fact that the O_2 effect on ΦPSII/ΦCO_2 was much less pronounced in C_4 *A. semialata MDG* than in C_3 *A. semialata GMT*. Similar to the *Flaveria* and *Cleome* results, a significant interaction between O_2 concentration and time ($P \leq 0.001$ at both light intensities) was also observed in *Alloteropsis*, with 2% O_2 more significantly reducing ΦPSII/ΦCO_2 during the start of induction than towards the end.

Discussion

The presented experiments investigated the efficiency of photosynthesis during light induction in phylogenetically linked *Alloteropsis*, *Flaveria*, and *Cleome* C_3 and C_4 species. Steady state and photosynthetic induction responses to light were measured to evaluate relative differences between paired species – controlling for evolutionary distance allowed for better differentiation between the effects of photosynthetic pathway and species-specific variation. At the start of light induction C_4 species had greater lag in CO_2 assimilation than C_3 species in all three comparisons (Figure 5A), confirming that the activation of CO_2 assimilation is generally slower in C_4 photosynthesis within the studied genera. However, the underlying reasons for this difference appeared to be genus specific. In C_4 *Flaveria*, slower induction appeared to be explained at least in part by less efficient suppression of photorespiration, since 2% O_2 resulted in increased CO_2 assimilation and fewer transferred electrons per fixed CO_2 (Figure 6). Although decreased photorespiratory electron sinks were also observable in C_4 *Alloteropsis* and *Cleome* induction under 2% O_2, there were no concurrent increases in CO_2 assimilation (Figure 5A), implying alternative limiting factors were at play, such as C_3 cycle activation. In C_3 *Cleome* and both *Alloteropsis* species, 2% O_2 actually suppressed activation of CO_2 assimilation, suggesting that photorespiration may support the induction of photosynthesis in these species.

Slower activation of CO_2 assimilation during light induction in C_4 versus C_3 photosynthesis

In line with previously observed photosynthetic induction responses (Pearcy and Seemann, 1990; Pearcy, 1990; Sassenrath-Cole and Pearcy, 1992; Mott and Woodrow, 2000) a transient reduction in CO_2 assimilation relative to steady state was observed in all species during light induction, with a more pronounced effect found in C_4 species (Figure 5). Greater losses of photosynthetic efficiency have previously been observed in C_4 grown under dynamic light in comparison to C_3 species and linked to mechanisms involving photosynthetic induction (Kubásek et al., 2013). Further fluctuating light work on plants grown under constant light (including C_4 *F. bidentis*) has also shown an increased lag in CO_2 assimilation in C_4 compared to C_3 species following step-increases in light intensity (Li et al., 2021). Similarly, in a study comparing a selection of C_3 and C_4 grasses (Lee et al., 2022), a biphasic increase in assimilation during the low to high light transition was the most significant limitation in maize and big bluestem, again emphasizing the C_4 lag in CO_2 assimilation. However, both Li et al. (2021) and Lee et al. (2022) studies examined the efficiency of fully induced photosynthesis subsequently exposed to stepwise decreases and increases in light intensity, whereas the C_4 lag-time when activation starts from darkness or from prolonged periods of low light may be even more pronounced.

During darkness or low light periods, stomatal closure could subsequently restrict photosynthetic assimilation during light induction due to a lack of coordination between CO_2 influx and assimilation. However, g_{sw} appears to increase in tandem with decreases in C_i, so stomatal opening does not seem to be the major source of limitation (Figures 4C, F, I, L). The lower g_{sw} found in C_4 species during light induction is consistent with studies that show C_4 species to have lower stomatal conductance and greater water use efficiency (Way et al., 2014; McAusland et al., 2016). It is worth noting that C_4 monocots under dynamic light have been reported to have faster stomatal opening and closing than C_3 monocots and dicots (Ozeki et al., 2022) yet stomatal kinetics in C_4 *A. semialata MDG* instead appear to be slower, again emphasizing the importance of accounting for species or genus-specific phenomena. However, although CO_2 availability can affect CO_2 assimilation during induction, other biochemical limitations appeared to dominate the responses observed here, as discussed in more detail below. The different C_4 decarboxylase pathways found across the three C_4 species studied have distinct energetic demands per cell type. The NADP-ME subtype found in C_4 *F. bidentis* and NAD-ME subtype in C_4 *G. gynandra* require substantial transfer of reductant between M and BS cells (Ishikawa et al., 2016) and steeper metabolite gradients for CCM operation, whilst mixed NADP-ME-PEPCK CCM found in C_4 *A. semialata MDG* can meet ATP and NADPH requirements more cell autonomously (Yin and Struik, 2021). Modelling simulations indicate that reduced metabolite concentrations may be required to sustain this C_4 pathway (Wang et al., 2014a). The greater cell autonomy regarding energetic supply and demand found in C_4 *A. semialata MDG* could suggest a capacity for faster activation of photosynthetic assimilation, yet in the light induction experiments CO_2 assimilation in C_4 *A. semialata MDG* lagged behind the other C_4 species during the first ten minutes after starting light exposure (Figure 5A, B). In the following paragraphs we explore the different mechanisms underlying the slow activation of C_4 photosynthesis across the three genera.

Photorespiration during C_4 photosynthetic induction, disadvantageous or beneficial?

Reduced CO_2 assimilation during induction in C_4 species has been hypothesised to derive from the need to build up C_4 cycle intermediates leading to a lag in the efficient suppression of photorespiration (Sage and Mckown, 2006). If so, induction in C_4 species when the photorespiratory pathway is suppressed by low O_2 should result in an increase in photosynthetic carbon assimilation. This appeared to be confirmed in C_4 *F. bidentis*, where CO_2 assimilation during induction was higher under 2% O_2 than under 21% O_2 (Figure 5), in contrast to CO_2 assimilation in C_4 *F. bidentis* under steady state which showed no difference in A_{CO2} between O_2 concentrations (Figures 2A, D and Table 1). Comparatively, the lack of an equivalent improvement in CO_2 assimilation under 2% O_2 in C_4 *A. semialata GMT* and C_4 *G. gynandra* suggests that in these species the activation of the C_3 cycle (Sassenrath-Cole and Pearcy, 1992; Mott and Woodrow, 2000) could instead be the limiting factor.

Surprisingly, despite the stimulating effect of 2% O_2 on steady state CO_2 assimilation in C_3 *A. semialata GMT* and C_3 *T. hassleriana*, and lack of O_2 sensitivity in C_4 *A. semialata GMT* (Figures 2A, D and Table 1), CO_2 assimilation in all three species during the first 10 min of light induction was lower in 2% O_2 than in 21% O_2 (Figures 5A, B). Reverse sensitivity to O_2 in C_3 species has been linked to limitation by the rate of triose phosphate utilisation (TPU) (Sharkey, 1985). Low O_2 suppresses the net export of photorespiratory intermediates serine or glycine and limits endogenous pools of inorganic phosphate (P_i), as the amino acids come from phosphorylated plastidic metabolites that when used up in the cytosol liberate P_i otherwise used in the glycerate-PGA conversion (McClain and Sharkey, 2019). Additionally, reduced rates of starch biosynthesis from triose phosphates, and phosphoglucose isomerase inhibition have been found in low O_2 conditions (Dietz, 1985). The lower CO_2 assimilation observed in 2% O_2

compared to 21% O_2 during induction in C_3 *A. semialata GMT* and C_3 *T. hassleriana* could thus be due to 2% O_2 causing suboptimal stromal phosphate levels, thereby transiently exacerbating TPU limitation. It remains unclear whether C_4 species suffer from TPU limitation (Zhou et al., 2019), or whether alternative mechanisms may be involved.

The photorespiratory pathway has previously been suggested to help prime the C_4 cycle by providing a carbon source from which to build C_3 and C_4 metabolite pools (Kromdijk et al., 2014; Stitt and Zhu, 2014; Schlüter and Weber, 2020; Fu and Walker, 2022; Medeiros et al., 2022). In C_4 species, photorespiration could help establish CCM metabolic gradients through interconversion of 3-phosphoglyceric acid (3-PGA) and PEP (Arrivault et al., 2016), and in plants with NADP-ME decarboxylase, such as mixed subtype NADP-ME PEPCK C_4 *A. semialata GMT*, models suggest photorespiration could support the activation of redox-regulated C_3 enzymes and contribute to the formation of C_3 cycle intermediates in the BS through the triose phosphate transporter (TPT) (Weber and Von Caemmerer, 2010; Wang et al., 2014b). In C_3 photosynthesis, beyond its photoprotective role (Kozaki and Takeba, 1996), photorespiration has been shown to enhance CO_2 fixation through the assimilation of nitrogen (Busch et al., 2018). A recent metabolomic analysis in maize suggested that photorespiratory intermediates may also provide this supporting role in C_4 species (Medeiros et al., 2022).

Decoupling between electron transport and photosynthesis: Alternative electron sinks and BS leakiness

Particularly at the start of light induction, C_3 and C_4 species had significantly higher $\Phi PSII/\Phi CO_2$ ratios (Figure 6) than during steady state measurements (Table 1), indicating less of the reducing power of the electron transport chain was going towards photosynthetic carbon fixation. This was particularly prominent in the C_4 species, both in absolute values and relative to steady state, where C_4 plants had either lower (C_4 *Alloteropsis* and *Flaveria*) or equal (C_4 *Cleome*) $\Phi PSII/\Phi CO_2$ values compared to their C_3 counterparts. The build-up of metabolite pools to establish sufficient concentration gradients between M and BS cells required for the efficient operation of C_4 photosynthesis seems a likely contributing factor increasing $\Phi PSII/\Phi CO_2$ ratios in C_4 photosynthesis. However, the change in ratio could also be due to a variety of alternative electron sinks having greater presence during induction and drawing electrons away from the C_3 cycle.

Not surprisingly, reductions in $\Phi PSII/\Phi CO_2$ ratio under 2% O_2 were observed in all C_3 species as well as in C_4 *F. bidentis*, showing the importance of photorespiration as an electron sink. Although a gradual decrease in $\Phi PSII/\Phi CO_2$ across time was observed during induction in both *Alloteropsis* and *Cleome* C_4 species (Figure 5), in contrast to C_4 *F. bidentis* the temporal changes were not O_2 sensitive. An alternative electron sink to photorespiration could be the Mehler reaction, which reduces O_2 in the chloroplast to hydrogen peroxide and has been suggested to play a role in C_3 and C_4 photosynthesis (Sagun et al., 2021). Suppression of the Mehler reaction under 2% O_2 could be consistent with the small reductions in CO_2 assimilation observed in both *Alloteropsis* species and C3 *T. hassleriana*, as the Mehler reaction supports ATP formation and the activity of related enzymes has been found to increase when photosynthesis is impaired (Fryer et al., 1998). However, evidence to support a significant contribution of the Mehler reaction to high rates of photosynthesis in both C_3 and C_4 species is generally lacking (Driever and Baker, 2011).

A transient increase in BS leakiness could be an alternative contributing factor to the elevated energetic cost of CO_2 assimilation during induction in C_4 *A. semialata* and C_4 *G. gynandra* that accounts for the lack of O_2 sensitivity. A lag in activation of the C_3 cycle following light exposure would result in an imbalance between the C_3 and C_4 cycles and greater leakage of CO_2 from the BS due to the CCM over-pumping, reducing quantum efficiency by requiring more ATP per CO_2 fixed (Kromdijk et al., 2014, Sage and McKown, 2006). Transient isotope discrimination measurements on sorghum and maize during the first 10 min following a step-increase in light intensity suggested that bundle sheath leakiness could be 60% higher than steady state (Kubásek et al., 2013; Wang et al., 2022) and remain elevated for up to 30 min. This seems consistent with the timing of the decrease in $\Phi PSII/\Phi CO_2$ during induction in the *Alloteropsis* and *Cleome* C_4 species. Thus, activation of CO_2 assimilation in these species may be limited by activation of the C_3 cycle, whereas the stable $\Phi PSII/\Phi CO_2$ values in C_4 *F. bidentis* under 2% O_2 suggest C_3 cycle activation is faster than the CCM in this species.

Conclusion

This study confirms C_4 photosynthesis experiences greater lag than C_3 photosynthesis during light induction – the greater depression of CO_2 assimilation in C_4 species was independently found in three evolutionary divergent comparisons of phylogenetically linked C_3 and C_4 species, providing experimental support for previous hypotheses and observations of less efficient photosynthetic induction in C_4 photosynthesis (Sage and Mckown, 2006; Kubásek et al., 2013; Slattery et al., 2018; Li et al., 2021; Sales et al., 2021). Despite the generally slower induction of CO_2 assimilation found in all C_4 species in comparison to their C_3 pairs, the underlying mechanisms to explain these differences were distinctly different – less effective suppression of photorespiration

seemed to underlie the reduction in CO_2 assimilation in C_4 *Flaveria* whereas delayed activation of the C_3 cycle appeared to be the limiting factor in C_4 species in *Alloteropsis* and *Cleome*, where a potential supporting role for photorespiration in photosynthetic induction was also identified. The substantial variation observed between and across phylogenetic pairs during both steady state and light induction measurements underscores the crucial importance of controlling for evolutionary distance when studying differences between photosynthetic pathways.

Data availability statement

The raw data supporting the conclusions of this article will be made available by the authors, without undue reservation.

Author contributions

JK conceived the study. JK, LAC and ACB designed the experiments. LAC carried out all experiments, data analysis and interpretation, and drafted the manuscript. RLV helped with the 2% O_2 experimental setup and provided support with gas exchange experiments. ELB procured the initial plant material. CRGS helped with data interpretation. All authors contributed to the article and approved the submitted version.

Funding

LAC was jointly funded by The Cambridge Commonwealth, European & International Trust; and by Mexico's Consejo Nacional de Ciencia y Tecnología (CONACyT).

Acknowledgments

The authors wish to thank Dr. Pascal-Antoine Christin at The University of Sheffield, Dr. Marjorie Lundgren at Lancaster Environmental Centre, and Prof. Peter Westhoff at Heinrich Heine University Düsseldorf for providing *A. semialata GMT* and *MDG* accessions, *F. cronquistii* cuttings, and *F. bidentis* seeds, respectively. For the purpose of open access, the author has applied a Creative Commons Attribution (CC BY) license to any Author Accepted Manuscript version arising from this submission.

Conflict of interest

The authors declare that the research was conducted in the absence of any commercial or financial relationships that could be construed as a potential conflict of interest.

Publisher's note

All claims expressed in this article are solely those of the authors and do not necessarily represent those of their affiliated organizations, or those of the publisher, the editors and the reviewers. Any product that may be evaluated in this article, or claim that may be made by its manufacturer, is not guaranteed or endorsed by the publisher.

Supplementary material

The Supplementary Material for this article can be found online at: https://www.frontiersin.org/articles/10.3389/fpls.2022.1091115/full#supplementary-material

References

Arrivault, S., Obata, T., Szecówka, M., Mengin, V., Guenther, M., Hoehne, M., et al. (2016). Metabolite pools and carbon flow during C4 photosynthesis in maize: 13CO2 labeling kinetics and cell type fractionation. *J. Exp. Bot.* 68, 283–298. doi: 10.1093/jxb/erw414

Bates, D., Mächler, M., Bolker, B., and Walker, S. (2015). Fitting linear mixed-effects models using lme4. *J. Stat. Software* 67, 1–48. doi: 10.18637/jss.v067.i01

Bräutigam, A., Kajala, K., Wullenweber, J., Sommer, M., Gagneul, D., Weber, K. L., et al. (2010). An mRNA blueprint for C4 photosynthesis derived from comparative transcriptomics of closely related C3 and C4 species. *Plant Physiol.* 155, 142–156. doi: 10.1104/pp.110.159442

Busch, F. A., Sage, R. F., and Farquhar, G. D. (2018). Plants increase CO2 uptake by assimilating nitrogen *via* the photorespiratory pathway. *Nat. Plants* 4, 46–54. doi: 10.1038/s41477-017-0065-x

Christin, P.-A., Osborne, C. P., Sage, R. F., Arakaki, M., and Edwards, E. J. (2011). C4 eudicots are not younger than C4 monocots. *J. Exp. Bot.* 62, 3171–3181. doi: 10.1093/jxb/err041

Dietz, K.-J. (1985). A possible rate-limiting function of chloroplast hexosemonophosphate isomerase in starch synthesis of leaves. *Biochim. Biophys. Acta (BBA) - Gen. Subj.* 839, 240–248. doi: 10.1016/0304-4165(85)90004-2

Driever, S. M., and Baker, N. R. (2011). The water-water cycle in leaves is not a major alternative electron sink for dissipation of excess excitation energy when CO2 assimilation is restricted. *Plant Cell Environ.* 34, 837–846. doi: 10.1111/j.1365-3040.2011.02288.x

FAO (2020). "Production, trade and prices of commodities," in *World food and agriculture - statistical yearbook 2020* (Rome, Italy: FAO).

Fryer, M. J., Andrews, J. R., Oxborough, K., Blowers, D. A., and Baker, N. R. (1998). Relationship between CO2 assimilation, photosynthetic electron transport, and active O2 metabolism in leaves of maize in the field during periods of low temperature. *Plant Physiol.* 116, 571–580. doi: 10.1104/pp.116.2.571

Fu, X., and Walker, B. J. (2022). Dynamic response of photorespiration in fluctuating light environments. *J. Exp. Botany*. doi: 10.1093/jxb/erac335

Genty, B., Briantais, J.-M., and Baker, N. R. (1989). The relationship between the quantum yield of photosynthetic electron transport and quenching of chlorophyll fluorescence. *Biochim. Biophys. Acta (BBA) - Gen. Subj.* 990, 87–92. doi: 10.1016/S0304-4165(89)80016-9

Gowik, U., Bräutigam, A., Weber, K. L., Weber, A. P. M., and Westhoff, P. (2011). Evolution of C4 photosynthesis in the genus *Flaveria*: How many and which genes does it take to make C4? *Plant Cell* 23, 2087–2105. doi: 10.1105/tpc.111.086264

Hatch, M., Kagawa, T., and Craig, S. (1975). Subdivision of C4-pathway species based on differing C4 acid decarboxylating systems and ultrastructural features. *Funct. Plant Biol.* 2, 111–128. doi: 10.1071/PP9750111

Ibrahim, D. G., Burke, T., Ripley, B. S., and Osborne, C. P. (2009). A molecular phylogeny of the genus *Alloteropsis* (Panicoideae, Poaceae) suggests an evolutionary reversion from C4 to C3 photosynthesis. *Ann. Bot.* 103, 127–136. doi: 10.1093/aob/mcn204

Ishikawa, N., Takabayashi, A., Sato, F., and Endo, T. (2016). Accumulation of the components of cyclic electron flow around photosystem I in C_4 plants, with respect to the requirements for ATP. *Photosynthesis Res.* 129, 261–277. doi: 10.1007/s11120-016-0251-0

Jawień, W. (2014). Searching for an optimal AUC estimation method: a never-ending task? *J. Pharmacokinet. Pharmacodynamics* 41, 655–673. doi: 10.1007/s10928-014-9392-y

Kellogg, E. A. (2013). C4 photosynthesis. *Curr. Biol.* 23, R594–R599. doi: 10.1016/j.cub.2013.04.066

Kok, B. (1949). On the interrelation of respiration and photosynthesis in green plants. *Biochimica et Biophysica Acta* 3, 625–631. doi: 10.1016/0006-3002(49)90136-5

Kozaki, A., and Takeba, G. (1996). Photorespiration protects C3 plants from photooxidation. *Nature* 384, 557–560. doi: 10.1038/384557a0

Krall, J. P., and Edwards, G. E. (1990). Quantum yields of photosystem II electron transport and carbon dioxide fixation in C4 plants. *Aust. J. Plant Physiol.* 17, 579–588. doi: 10.1071/PP9900579

Kromdijk, J., Griffiths, H., and Schepers, H. E. (2010). Can the progressive increase of C_4 bundle sheath leakiness at low PFD be explained by incomplete suppression of photorespiration? *Plant Cell Environ.* 33, 1935–1948. doi: 10.1111/j.1365-3040.2010.02196.x

Kromdijk, J., Ubierna, N., Cousins, A. B., and Griffiths, H. (2014). Bundle-sheath leakiness in C4 photosynthesis: a careful balancing act between CO2 concentration and assimilation. *J. Exp. Bot.* 65, 3443–3457. doi: 10.1093/jxb/eru157

Kubásek, J., Urban, O., and Šantrůček, J. (2013). C4 plants use fluctuating light less efficiently than do C3 plants: a study of growth, photosynthesis and carbon isotope discrimination. *Physiologia Plantarum* 149, 528–539. doi: 10.1111/ppl.12057

Kuznetsova, A., Brockhoff, P. B., and Christensen, R. H. B. (2017). lmerTest package: Tests in linear mixed effects models. *J. Stat. Software* 821–26. doi: 10.18637/jss.v082.i13

Lee, M. S., Boyd, R. A., and Ort, D. R. (2022). The photosynthetic response of C3 and C4 bioenergy grass species to fluctuating light. *GCB Bioenergy* 14, 37–53. doi: 10.1111/gcbb.12899

Leegood, R. C. (2002). C4 photosynthesis: principles of CO2 concentration and prospects for its introduction into C3 plants. *J. Exp. Bot.* 53, 581–590. doi: 10.1093/jexbot/53.369.581

Leegood, R. C., and Furbank, R. T. (1984). Carbon metabolism and gas exchange in leaves of *Zea* mays l. *Planta* 162, 450–456. doi: 10.1007/BF00393458

Li-Cor, I. (1988). *1800-12 integrating sphere instruction manual*. LI-COR.: Lincoln, Nebraska.

Li, Y.-T., Luo, J., Liu, P., and Zhang, Z.-S. (2021). C4 species utilize fluctuating light less efficiently than C3 species. *Plant Physiol.* 187, 1288–1291. doi: 10.1093/plphys/kiab411

Loriaux, S. D., Avenson, T. J., Welles, J. M., Mcdermitt, D. K., Eckles, R. D., Riensche, B., et al. (2013). Closing in on maximum yield of chlorophyll fluorescence using a single multiphase flash of sub-saturating intensity. *Plant Cell Environ.* 36, 1755–1770. doi: 10.1111/pce.12115

Lundgren, M. R., Besnard, G., Ripley, B. S., Lehmann, C. E. R., Chatelet, D. S., Kynast, R. G., et al. (2015). Photosynthetic innovation broadens the niche within a single species. *Ecol. Lett.* 18, 1021–1029. doi: 10.1111/ele.12484

Lyu, M.-J. A., Gowik, U., Kelly, S., Covshoff, S., Mallmann, J., Westhoff, P., et al. (2015). RNA-Seq based phylogeny recapitulates previous phylogeny of the genus flaveria (Asteraceae) with some modifications. *BMC Evolutionary Biol.* 15, 116. doi: 10.1186/s12862-015-0399-9

Makowski, D., Ben-Shachar, M. S., and Lüdecke, D. (2019). bayestestR: Describing effects and their uncertainty, existence and significance within the Bayesian framework. *J. Open Source Software* 4, 40. doi: 10.21105/joss.01541

McAusland, L., Vialet-Chabrand, S., Davey, P., Baker, N. R., Brendel, O., and Lawson, T. (2016). Effects of kinetics of light-induced stomatal responses on photosynthesis and water-use efficiency. *New Phytol.* 211, 1209–1220. doi: 10.1111/nph.14000

McClain, A. M., and Sharkey, T. D. (2019). Triose phosphate utilization and beyond: from photosynthesis to end product synthesis. *J. Exp. Bot.* 70, 1755–1766. doi: 10.1093/jxb/erz058

Medeiros, D. B., Ishihara, H., Guenther, M., Rosado De Souza, L., Fernie, A. R., Stitt, M., et al. (2022). 13CO2 labeling kinetics in maize reveal impaired efficiency of C4 photosynthesis under low irradiance. *Plant Physiol.* 190, 280–304. doi: 10.1093/plphys/kiac306

Mott, K. A., and Woodrow, I. E. (2000). Modelling the role of rubisco activase in limiting non-steady-state photosynthesis. *J. Exp. Bot.* 51, 399–406. doi: 10.1093/jexbot/51.suppl_1.399

Neuwirth, E. (2014). *RColorBrewer: ColorBrewer palettes*.

Oberhuber, W., and Edwards, G. E. (1993). Temperature dependence of the linkage of quantum yield of photosystem II to CO2 fixation in C4 and C3 plants. *Plant Physiol.* 101, 507–512. doi: 10.1104/pp.101.2.507

Ozeki, K., Miyazawa, Y., and Sugiura, D. (2022). Rapid stomatal closure contributes to higher water use efficiency in major C_4 compared to C_3 Poaceae crops. *Plant Physiol.* 189, 188–203. doi: 10.1093/plphys/kiac040

Pearcy, R. W. (1990). Sunflecks and photosynthesis in plant canopies. *Annu. Rev. Plant Physiol. Plant Mol. Biol.* 41, 421–453. doi: 10.1146/annurev.pp.41.060190.002225

Pearcy, R. W., and Seemann, J. R. (1990). Photosynthetic induction state of leaves in a soybean canopy in relation to light regulation of ribulose-1-5-Bisphosphate carboxylase and stomatal conductance. *Plant Physiol.* 94, 628–633. doi: 10.1104/pp.94.2.628

R Core Team (2021). *R: A language and environment for statistical computing* (Vienna, Austria: R Foundation for Statistical Computing).

RStudio Team (2022). *RStudio: Integrated development environment for r* (Boston, MA: RStudio, PBC).

Sage, R. F. (2004). The evolution of C4 photosynthesis. *New Phytol.* 161, 341–370. doi: 10.1111/j.1469-8137.2004.00974.x

Sage, R. F., and McKown, A. D. (2006). Is C4 photosynthesis less phenotypically plastic than C3 photosynthesis? *J. Exp. Bot.* 57, 303–317. doi: 10.1093/jxb/erj040

Sagun, J. V., Badger, M. R., Chow, W. S., and Ghannoum, O. (2021). Mehler reaction plays a role in C_3 and C_4 photosynthesis under shade and low CO_2. *Photosynthesis Res.* 149, 171–185. doi: 10.1007/s11120-021-00819-1

Sales, C. R. G., Wang, Y., Evers, J. B., and Kromdijk, J. (2021). Improving C4 photosynthesis to increase productivity under optimal and suboptimal conditions. *J. Exp. Bot.* 72, 5942–5960. doi: 10.1093/jxb/erab327

Sassenrath-Cole, G. F., and Pearcy, R. W. (1992). The role of ribulose-1,5-Bisphosphate regeneration in the induction requirement of photosynthetic CO_2 exchange under transient light conditions. *Plant Physiol.* 99, 227–234. doi: 10.1104/pp.99.1.227

Schlüter, U., and Weber, A. P. M. (2020). Regulation and evolution of C_4 photosynthesis. *Annu. Rev. Plant Biol.* 71, 183–215. doi: 10.1146/annurev-arplant-042916-040915

Sharkey, T. D. (1985). O_2-insensitive photosynthesis in C_3 plants: its occurrence and a possible explanation. *Plant Physiol.* 78, 71–75. doi: 10.1104/pp.78.1.71

Shi, D., Li, J., Li, Y., Li, Y., and Xie, L. (2021). The complete chloroplast genome sequence of *Gynandropsis gynandra* (Cleomaceae). *Mitochondrial* 6 (7), 1909–1910. doi: 10.1080/23802359.2021.1935339

Slattery, R. A., Walker, B. J., Weber, A. P. M., and Ort, D. R. (2018). The impacts of fluctuating light on crop performance. *Plant Physiol.* 176, 990–1003. doi: 10.1104/pp.17.01234

Still, C. J., Berry, J. A., Collatz, G. J., and Defries, R. S. (2003). Global distribution of C3 and C4 vegetation: Carbon cycle implications. *Global Biogeochemical Cycles* 17, 6–1-6-14. doi: 10.1029/2001gb001807

Stinziano, J. R., Roback, C., Sargent, D., Murphy, B. K., Hudson, P. J., and Muir, C. D. (2021). Principles of resilient coding for plant ecophysiologists. *AoB PLANTS* 13. doi: 10.1093/aobpla/plab059

Stitt, M., and Zhu, X.-G. (2014). The large pools of metabolites involved in intercellular metabolite shuttles in C4 photosynthesis provide enormous flexibility and robustness in a fluctuating light environment. *Plant Cell Environ.* 37, 1985–1988. doi: 10.1111/pce.12290

Taylor, S. H., Hulme, S. P., Rees, M., Ripley, B. S., Ian Woodward, F., and Osborne, C. P. (2010). Ecophysiological traits in C_3 and C_4 grasses: a phylogenetically controlled screening experiment. *New Phytol.* 185, 780–791. doi: 10.1111/j.1469-8137.2009.03102.x

Ueno, O., and Sentoku, N. (2006). Comparison of leaf structure and photosynthetic characteristics of C3 and C4 *Alloteropsis semialata* subspecies. *Plant Cell Environ.* 29, 257–268. doi: 10.1111/j.1365-3040.2005.01418.x

Usuda, H. (1985). Changes in levels of intermediates of the C_4 cycle and reductive pentose phosphate pathway during induction of photosynthesis in maize leaves. *Plant Physiol.* 78, 859–864. doi: 10.1104/pp.78.4.859

Wang, Y., Bräutigam, A., Weber, A. P. M., and Zhu, X.-G. (2014a). Three distinct biochemical subtypes of C4 photosynthesis? A modelling analysis. *J. Exp. Bot.* 65, 3567–3578. doi: 10.1093/jxb/eru058

Wang, C., Guo, L., Li, Y., and Wang, Z. (2012). Systematic comparison of C3 and C4 plants based on metabolic network analysis. *BMC Syst. Biol.* 6, S9. doi: 10.1186/1752-0509-6-S2-S9

Wang, Y., Long, S. P., and Zhu, X. G. (2014b). Elements required for an efficient NADP-malic enzyme type C4 photosynthesis. *Plant Physiol.* 164, 2231–2246. doi: 10.1104/pp.113.230284

Wang, Y., Stutz, S. S., Bernacchi, C. J., Boyd, R. A., Ort, D. R., and Long, S. P. (2022). Increased bundle-sheath leakiness of CO2 during photosynthetic induction shows a lack of coordination between the C4 and C4 cycles. *New Phytol.* 236, 1661–1675. doi: 10.1111/nph.18485

Way, D. A., Katul, G. G., Manzoni, S., and Vico, G. (2014). Increasing water use efficiency along the C_3 to C_4 evolutionary pathway: a stomatal optimization perspective. *J. Exp. Bot.* 65, 3683–3693. doi: 10.1093/jxb/eru205

Weber, A. P., and Von Caemmerer, S. (2010). Plastid transport and metabolism of C3 and C4 plants–comparative analysis and possible biotechnological exploitation. *Curr. Opin. Plant Biol.* 13, 257–265. doi: 10.1016/j.pbi.2010.01.007

Wickham, H., Averick, M., Bryan, J., Chang, W., Mcgowan, L., François, R., et al. (2019). Welcome to the tidyverse. *J. Open Source Software* 4, 1686. doi: 10.21105/joss.01686

Yin, X., and Struik, P. C. (2018). The energy budget in C4 photosynthesis: insights from a cell-type-specific electron transport model. *New Phytol.* 218, 986–998. doi: 10.1111/nph.15051

Yin, X., and Struik, P. C. (2021). Exploiting differences in the energy budget among C_4 subtypes to improve crop productivity. *New Phytol.* 229, 2400–2409. doi: 10.1111/nph.17011

Zelitch, I., Schultes, N. P., Peterson, R. B., Brown, P., and Brutnell, T. P. (2009). High glycolate oxidase activity is required for survival of maize in normal air. *Plant Physiol.* 149, 195–204. doi: 10.1104/pp.108.128439

Zhou, H., Akçay, E., and Helliker, B. R. (2019). Estimating C_4 photosynthesis parameters by fitting intensive A/C_i curves. *Photosynthesis Res.* 141, 181–194. doi: 10.1007/s11120-019-00619-8